degradation of polyethylene *in vivo* is related to the surrounding oxygen concentration, that is, that of the body fluid, it is not a main factor of the degradation as a whole. However, recent studies reported that conventional or cross-linked gamma-ray sterilized polyethylene liners undergo *in vivo* oxidation, especially in unworn bearing surface regions and the rim. In contrast, the oxidation of a worn bearing surface was not observed.[47] On the basis of these studies, we assumed that when oxygen is excluded from the package during sterilization, further cross-linking, and additional improvement in the wear performance are attained. However, we must pay attention to the rim fracture in CLPE-*g*-MPC cup by the possible impingements based on the abovementioned studies.[47] In the previous study, for gamma-ray irradiation, the lower molecular weight cross-linked GUR1020 materials had higher mechanical properties (tensile and impact properties) for all doses as compared to the higher molecular weight cross-linked GUR1050 materials.[48] Therefore, we selected a GUR1020 compression-molded bar stock as the CLPE substrate. Nevertheless, the cross-linked GUR1020 materials showed the same wear rate as the cross-linked GUR1050 materials.

Gamma-ray sterilization has had a long history and it has been one of the most popular sterilization methods for various medical products to date. A barrier package has been widely adopted to satisfactorily address the historical problem of the oxidation of gamma-ray sterilized products during shelf storage. In this study, we confirmed that the extra energy supplied by gamma-ray irradiation produced cross-linking in the three regions of the CLPE-*g*-MPC: poly(MPC) layer, CLPE-MPC interface, and CLPE substrate. When the CLPE surface is modified by poly(MPC) grafting, the MPC graft polymer leads to a significant reduction in the sliding friction between the surfaces which are grafted because water thin films formed can act as extremely efficient lubricants. Gamma-ray sterilized CLPE-*g*-MPC showed a slightly higher friction than the nonsterilized one. However, the wear resistance is more stable in the former than in the latter. The cross-links formed by gamma-ray irradiation would give further longevity to CLPE-*g*-MPC cups. Based on the mechanical,[19] biological,[5,49,50] and tribological advantages of MPC polymers, CLPE-*g*-MPC is believed to be promising for use in the next-generation artificial hip joint systems.

The authors also express special thanks to Dr. Masaru Ueno, Mr. Takatoshi Miyashita, and Mr. Noboru Yamawaki (Japan Medical Materials Corp.) for their excellent technical assistance.

REFERENCES

1. Kurtz S, Mowat F, Ong K, Chan N, Lau E, Halpern M. Prevalence of primary and revision total hip and knee arthroplasty in the United States from 1990 through 2002. J Bone Joint Surg Am 2005;87:1487–1497.
2. Harris WH. The problem is osteolysis. Clin Orthop 1995;311: 46–53.
3. Kobayashi A, Freeman MA, Bonfield W, Kadoya Y, Yamac T, Al-Saffar N, Scott G, Revell PA. Number of polyethylene particles and osteolysis in total joint replacements. A quantitative study using a tissue-digestion method. J Bone Joint Surg Br 1997;79:844–848.
4. Sochart DH. Relationship of acetabular wear to osteolysis and loosening in total hip arthroplasty. Clin Orthop 1999;363: 135–150.
5. Moro T, Takatori Y, Ishihara K, Konno T, Takigawa Y, Matsushita T, Chung UI, Nakamura K, Kawaguchi H. Surface grafting of artificial joints with a biocompatible polymer for preventing periprosthetic osteolysis. Nature Mater 2004;3: 829–837.
6. Moro T, Takatori Y, Ishihara K, Nakamura K, Kawaguchi H. Grafting of biocompatible polymer for longevity of artificial hip joints. Clin Orthop Relat Res 2006;453:58–63.
7. Kyomoto M, Moro T, Konno T, Takadama H, Yamawaki N, Kawaguchi H, Takatori Y, Nakamura K, Ishihara K. Enhanced wear resistance of modified cross-linked polyethylene by grafting with poly(2-methacryloyloxyethyl phosphorylcholine). J Biomed Mater Res A 2007;82:10–17.
8. Ishihara K, Ueda T, Nakabayashi N. Preparation of phospholipid polymers and their properties as polymer hydrogel membranes. Polym J 1990;22:355–360.
9. Sawada S, Iwasaki Y, Nakabayashi N, Ishihara K. Stress response of adherent cells on a polymer blend surface composed of a segmented polyurethane and MPC copolymers. J Biomed Mater Res A 2006;79:476–484.
10. Goda T, Konno T, Takai M, Moro T, Ishihara K. Biomimetic phosphorylcholine polymer grafting from polydimethylsiloxane surface using photo-induced polymerization. Biomaterials 2006;27:5151–5160.
11. Sibarani J, Takai M, Ishihara K. Surface modification on microfluidic devices with 2-methacryloyloxyethyl phosphorylcholine polymers for reducing unfavorable protein adsorption. Colloids Surf B Biointerfaces 2007;54:88–93.
12. Ueda H, Watanabe J, Konno T, Takai M, Saito A, Ishihara K. Asymmetrically functional surface properties on biocompatible phospholipid polymer membrane for bioartificial kidney. J Biomed Mater Res A 2006;77:19–27.
13. Bakhai A, Booth J, Delahunty N, Nugara F, Clayton T, McNeill J, Davies SW, Cumberland DC, Stables RH, SV Stent Investigators. The SV stent study: A prospective, multicentre, angiographic evaluation of the BiodivYsio phosphorylcholine coated small vessel stent in small coronary vessels. Int J Cardiol 2005;102:95–102.
14. Watanabe J, Ishihara K. Cell engineering biointerface focusing on cytocompatibility using phospholipid polymer with an isomeric oligo(lactic acid) segment. Biomacromolecules 2005; 6:1797–1802.
15. Abraham S, Brahim S, Ishihara K, Guiseppi-Elie A. Molecularly engineered p(HEMA)-based hydrogels for implant biochip biocompatibility. Biomaterials 2005;26:4767–4778.
16. Konno T, Hasuda H, Ishihara K, Ito Y. Photo-immobilization of a phospholipid polymer for surface modification. Biomaterials 2005;26:1381–1388.
17. Palmer RR, Lewis AL, Kirkwood LC, Rose SF, Lloyd AW, Vick TA, Stratford PW. Biological evaluation and drug delivery application of cationically modified phospholipid polymers. Biomaterials 2004;25:4785–4796.
18. Long SF, Clarke S, Davies MC, Lewis AL, Hanlon GW, Lloyd AW. Controlled biological response on blends of a phosphorylcholine-based copolymer with poly(butyl methacrylate). Biomaterials 2003;24:4115–4121.
19. Kyomoto M, Moro T, Konno T, Takadama H, Kawaguchi H, Takatori Y, Nakamura K, Yamawaki N, Ishihara K. Effects of photo-induced graft polymerization of 2-methacryloyloxyethyl phosphorylcholine on physical properties of cross-linked poly-

ethylene in artificial hip joints. J Mater Sci Mater Med, Forthcoming.
20. Costa L, Luda MP, Trossarelli L, Brach del Prever EM, Crova M, Gallinaro P. Oxidation in orthopaedic UHMWPE sterilized by gamma-ray radiation and ethylene oxide. Biomaterials 1998;19:659–668.
21. McKellop H, Shen FW, Lu B, Campbell P, Salovey R. Effect of sterilization method and other modifications on the wear resistance of acetabular cups made of ultra-high molecular weight polyethylene. A hip-simulator study. J Bone Joint Surg Am 2000;82:1708–1725.
22. Wang A, Sun DC, Yau SS, Edwards B, Sokol M, Essner A, Polineni VK, Stark C, Dumbleton JH. Orientation softening in the deformation and wear of ultra-high molecular weight polyethylene. Wear 1997;203–204:230–241.
23. Digas G, Thanner J, Nivbrant B, Rohrl S, Strom H, Karrholm J. Increase in early polyethylene wear after sterilization with ethylene oxide: Radiostereometric analyses of 201 total hips. Acta Orthop Scand 2003;74:531–541.
24. Manning DW, Chiang PP, Martell JM, Galante JO, Harris WH. In vivo comparative wear study of traditional and highly cross-linked polyethylene in total hip arthroplasty. J Arthroplasty 2005;20:880–886.
25. Ishihara K, Iwasaki Y, Ebihara S, Shindo Y, Nakabayashi N. Photoinduced graft polymerization of 2-methacryloyloxyethyl phosphorylcholine on polyethylene membrane surface for obtaining blood cell adhesion resistance. Colloids Surf B 2000;18:325–335.
26. International Organization for Standardization 15989. Plastics–Film and sheeting–Measurement of water-contact angle of corona-treated films, Geneva, 2004.
27. International Organization for Standardization 14242–1. Implants for surgery–Wear of total hip-joint prostheses–Part 1: Loading and displacement parameters for wear-testing machines and corresponding environmental conditions for test, 2002.
28. International Organization for Standardization 14242–2. Implants for surgery–Wear of total hip-joint prostheses–Part 2: Methods of measurement, 2000.
29. Saikko V. Wear and friction properties of prosthetic joint materials evaluated on a reciprocating pin-on-flat apparatus. Wear 1993;166:169–178.
30. Yao JQ, Laurent MP, Johnson TS, Blanchard CR, Crowninshield RD. The influences of lubricant and material on polymer/CoCr sliding friction. Wear 2003;255:780–784.
31. Bracco P, Brunella V, Luda MP, Brach del Prever EM, Zanetti M, Costa L. Oxidation behaviour in prosthetic UHMWPE components sterilised with high energy radiation in a low-oxygen environment. Polym Degrad Stab 2006;91: 3057–3064.
32. Premnath V, Harris WH, Jasty M, Merrill EW. Gamma sterilization of UHMWPE articular implants: An analysis of the oxidation problem. Ultra high molecular weight poly ethylene. Biomaterials 1996;17:1741–1753.
33. de Vicente J, Stokes JR, Spikes HA. Soft lubrication of model hydrocolloids. Food Hydrocolloids 2006;20:483–491.
34. Raviv U, Frey J, Sak R, Laurat P, Tadmor R, Klein J. Properties and interactions of physigrafted end-functionalized poly (ethylene glycol) layers. Langmuir 2002;18:7482–7495.
35. Raviv U, Glasson S, Kampf N, Gohy JF, Jérôme R, Klein J. Lubrication by charged polymers. Nature 2003;425:163–165.
36. Salleh NG, Glasel HJ, Mehnert R. Development of hard materials by radiation curing technology. Radiat Phys Chem 2002;63:475–479.
37. Lewis AL, Cumming ZL, Goreish HH, Kirkwood LC, Tolhurst LA, Stratford PW. Crosslinkable coatings from phosphorylcholine-based polymers. Biomaterials 2001;22:99–111.
38. McKellop H, Shen FW, Lu B, Campbell P, Salovey R. Development of an extremely wear-resistant ultra high molecular weight polyethylene for total hip replacements. J Orthop Res 1999;17:157–167.
39. Muratoglu OK, Bragdon CR, O'Connor DO, Jasty M, Harris WH. A novel method of crosslinking ultra-high-molecular-weight polyethylene to improve wear, reduce oxidation, and retain mechanical properties. Recipient of the 1999 HAP Paul Award. J Arthroplasty 2001;16:149–160.
40. Oonishi H, Kim SC, Takao Y, Kyomoto M, Iwamoto M, Ueno M. Wear of highly cross-linked polyethylene acetabular cup in Japan. J Arthroplasty 2006;21:944–949.
41. Dowson D, Jin ZM. Micro-elastohydrodynamic lubrication of synovial joints. Eng Med 1986;15:63–65.
42. Williams PF III, Powell GL, LaBerge M. Sliding friction analysis of phosphatidylcholine as a boundary lubricant for articular cartilage. Proc Inst Mech Eng [H] 1993;207:59–66.
43. Willie BM, Ashrafi S, Alajbegovic S, Burnett T, Bloebaum RD. Quantifying the effect of resin type and sterilization method on the degradation of ultrahigh molecular weight polyethylene after 4 years of real-time shelf aging. J Biomed Mater Res A 2004;69:477–489.
44. Kurtz SM, Rimnac CM, Hozack WJ, Turner J, Marcolongo M, Goldberg VM, Kraay MJ, Edidin AA. In vivo degradation of polyethylene liners after gamma-ray sterilization in air. J Bone Joint Surg Am 2005;87:815–823.
45. Kyomoto M, Ueno M, Kim SC, Oonishi H, Oonishi H. Wear of "100 Mrad" cross-linked polyethylene: Effects of packaging after 30 years real-time shelf-aging. J Biomed Sci Polym Edn 2007;18:59–70.
46. Treuhaft PS, McCarty DJ. Synovial fluid pH, lactate, oxygen and carbon dioxide partial pressure in various joint diseases. Arthritis Rheum 1971;14:475–484.
47. Kurtz SM, Hozack W, Turner J, Purtill J, MacDonald D, Sharkey P, Parvizi J, Manley M, Rothman R. Mechanical properties of retrieved highly cross-linked crossfire liners after short-term implantation. J Arthroplasty 2005;20:840–849.
48. Greer KW, King RS, Chan FW. The effects of raw material, irradiation dose, and irradiation source on crosslinking of UHMWPE. In: Kurtz SM, Gsell RA, Martell J, editors. Cross-linked and thermally treated ultra-high molecular weight polyethylene for joint replacements. West Conshohocken: American Society for Testing and Materials; 2003. pp 209–220.
49. Ishihara K, Aragaki R, Ueda T, Watanabe A, Nakabayashi N. Reduced thrombogenicity of polymers having phospholipid polar groups. J Biomed Mater Res 1990;24:1069–1077.
50. Ishihara K, Ziats NP, Tierney BP, Nakabayashi N, Anderson JM. Protein adsorption from human plasma is reduced on phospholipids polymers. J Biomed Mater Res 1991;25:1397–1407.

Erratum

Enhanced Wear Resistance of Orthopaedic Bearing Due to the Cross-Linking of Poly(MPC) Graft Chains Induced by Gamma-Ray Irradiation

Masayuki Kyomoto,[1,2] Toru Moro,[3] Fumiaki Miyaji,[1] Tomohiro Konno,[2] Masami Hashimoto,[4] Hiroshi Kawaguchi,[3] Yoshio Takatori,[3] Kozo Nakamura,[3] Kazuhiko Ishihara[2]

[1] Research Division, Japan Medical Materials Corporation, Osaka, Japan

[2] Department of Materials Engineering, School of Engineering and Center for NanoBio Integration, The University of Tokyo, Tokyo, Japan

[3] Department of Orthopaedic Surgery, School of Medicine, The University of Tokyo, Tokyo, Japan

[4] Materials Research and Development Laboratory, Japan Fine Ceramics Center, Nagoya, Japan

Received 17 January 2007; revised 31 March 2007; accepted 30 April 2007
Published online 22 June 2007 in Wiley InterScience (www.interscience.wiley.com). DOI: 10.1002/jbm.b.30874
Erratum published online 20 February 2008 in Wiley InterScience (www.interscience.wiley.com). DOI: 10.1002/jbm.b.31079

The authors have requested the following revisions for the article listed above, published in J Biomed Mater Res B Appl Biomater 2008; 84B: 320–327. The updated Figures 3 and 4 appear below. The authors regret any confusion caused by these errors.

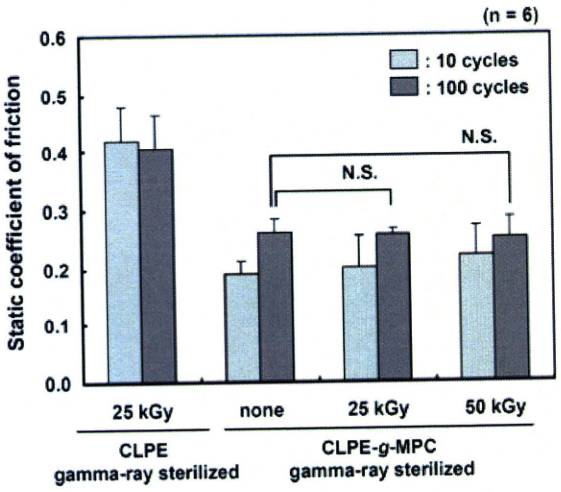

Figure 3. Static coefficients of friction of the gamma-ray sterilized CLPE surfaces and nonsterilized and gamma-ray sterilized CLPE-*g*-MPC surfaces. Bar, Standard deviations.

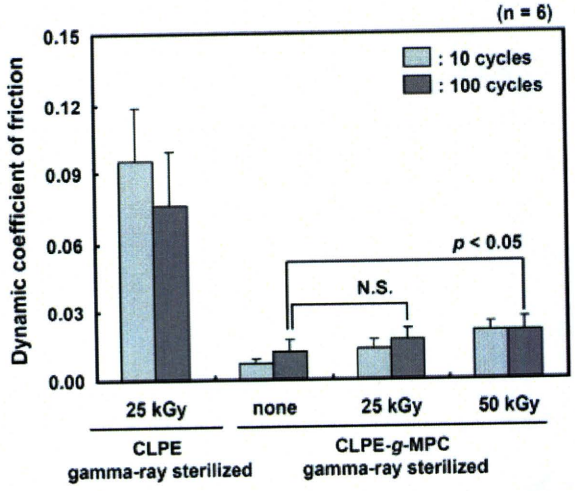

Figure 4. Dynamic coefficients of friction of gamma-ray sterilized CLPE surfaces and nonsterilized and gamma-ray sterilized CLPE-*g*-MPC surfaces. Bar, Standard deviations.

Effect of 2-methacryloyloxyethyl phosphorylcholine concentration on photo-induced graft polymerization of polyethylene in reducing the wear of orthopaedic bearing surface

Masayuki Kyomoto,[1,2] Toru Moro,[3] Fumiaki Miyaji,[1] Masami Hashimoto,[4] Hiroshi Kawaguchi,[3] Yoshio Takatori,[3] Kozo Nakamura,[3] Kazuhiko Ishihara[2]

[1]*Research Department, Japan Medical Materials Corporation, Osaka, Japan*

[2]*Department of Materials Engineering, School of Engineering and Center for NanoBio Integration, The University of Tokyo, Tokyo, Japan*

[3]*Department of Orthopaedic Surgery, School of Medicine, The University of Tokyo, Tokyo, Japan*

[4]*Materials Research and Development Laboratory, Japan Fine Ceramics Center, Nagoya, Japan*

Received 23 April 2007; accepted 15 May 2007
Published online 1 November 2007 in Wiley InterScience (www.interscience.wiley.com). DOI: 10.1002/jbm.a.31511

Abstract: Photo-induced graft polymerization of 2-methacryloyloxyethyl phosphorylcholine (MPC) on cross-linked polyethylene (CLPE) has been developed as a novel technology for reducing wear of orthopaedic bearings. In this study, the effect of MPC concentration on graft polymerization and the resultant properties of the grafted poly (MPC) layer have been investigated. The grafted poly (MPC) layer thickness increased with the MPC concentration in feed. The hip simulator wear test confirmed that CLPE-*g*-MPC cups exhibited minimal wear compared with untreated CLPE cups. Since MPC is a highly hydrophilic methacrylate, the water-wettability of CLPE-*g*-MPC was greater than that of untreated CLPE due to the formation of a poly(MPC) nanometer-scale layer. The CLPE-*g*-MPC orthopaedic bearing surface exhibited high lubricity, because of the present of the poly(MPC) layer even at a thickness of 10 nm. This layer is considered responsible for the improved wear resistance. Nanometer-scale modification of CLPE with poly(MPC) is expected to significantly increase the durability of the orthopaedic bearings. Poly (MPC) layer thickness can be controlled by changing the MPC concentration in feed. In order to achieve nanometer-scale modification of poly(MPC) in this manner, it is necessary to use a long photo-irradiation time for the MPC graft polymerization system, which contains a high-concentration monomer without its gelation. © 2007 Wiley Periodicals, Inc. J Biomed Mater Res 86A: 439–447, 2008

Key words: joint replacement; polyethylene; phosphorylcholine; graft polymerization; wear mechanism

INTRODUCTION

Polymeric biomaterials are widely used in the biomedical field for manufacturing artificial organs, medical devices, and disposable clinical apparatus.[1,2] The number of artificial hip and knee joints used for primary and revised hip and knee replacement are substantially increasing in the worldwide every year.[3] This indicates that the quality of medical devices such as artificial joints has become increasingly important. The most popular artificial joint system used as a medical device is a bearing couple composed of ultra-high molecular weight polyethylene (UHMWPE) and cobalt–chromium–molybdenum (Co-Cr-Mo) alloy. However, osteolysis caused by the wear particles of UHMWPE in the artificial joint system has emerged as a serious issue.[4,5] Different combinations of bearing surfaces and improvements in bearing materials have been studied with the aim of reducing the number of UHMWPE wear particles inducing osteolysis.[6–9]

Surface modification is important for the improvement of bearing materials. Recently, we developed an artificial hip joint based on a new concept by using 2-methacryloyloxyethyl phosphorylcholine (MPC) polymer grafted onto the surface of cross-linked polyethylene (CLPE; CLPE-*g*-MPC); this device was designed to reduce wear and suppress bone resorp-

Correspondence to: M. Kyomoto; e-mail: kyomotom@jmmc.jp

Contract grant sponsor: Japanese Ministry of Education, Culture, Sports, Science and Technology; contract grant number: 15390449
Contract grant sponsor: Japanese Ministry of Health, Labour and Welfare (Health and Welfare Research Grant)

tion.[10–13] MPC, a methacrylate monomer with a phospholipid polar group in the side chain, is a novel biomaterial designed and developed by Ishihara et al., and it mimics the neutral phospholipids of cell membranes.[14] MPC polymers are one of the most common biocompatible and hydrophilic polymers studied thus far, which have potential application in a variety of fields such as biology, biomedical science, and surface chemistry because they possess the unique properties of good biocompatibility, high lubricity and low friction, anti-protein adsorption, and cell membrane-like surface.[15–22]

In general, there are two methods for modifying the polymer surface. The first method involves surface absorption or reaction with small molecules[23–25] and the second, grafting polymeric molecules onto the substrate through covalent bonding.[26] Most frequently, grafting polymerization is performed using either of the following methods: (1) surface-initiated graft polymerization termed as the "grafting from" method in which the monomers are polymerized from initiators or comonomers; and (2) adsorption of the polymer to the substrate termed as the "grafting to" methods (i.e., dipping, cross-linking, and ready-made polymers with reactive end groups reacting with the functional groups of the substrate).[27,28] The "grafting from" method has an advantage over the "grafting to" method in that it synthesizes a high-density polymer brush. The novel artificial joint developed in this study is low-wear bearing with nanometer-scale poly(MPC) surface modification. This surface modification was accomplished by using a photo-induced radical polymerization technique that was similar to that used in the "grafting from" method. However, in this technique, controlling the length and density of the grafted poly(MPC) was difficult.[15] Our previous study confirmed that the density of the grafted poly(MPC) affects wear resistance and that it was controlled by the photo-irradiation time.[12]

In an attempt to resolve another issue in this study, we investigated the effect of MPC concentration variability on photo-induced graft polymerization. The results revealed that it was possible to control the grafted poly(MPC) chains with nanometer scale modification in order to reduce wear of the CLPE-*g*-MPC orthopaedic bearing surface.

MATERIALS AND METHODS

Chemicals

Benzophenone and acetone were purchased from Wako Pure Chemical Industries, (Osaka, Japan). MPC was industrially synthesized using the method reported by Ishihara et al.[14] and supplied by Ai Bio-Chips, (Tokyo, Japan).

MPC graft polymerization

A compression-molded UHMWPE (GUR1020 resin; Poly Hi Solidur, IN, USA) bar stock was irradiated with gamma-ray of 50 kGy in N_2 gas and annealed at 120°C for 7.5 h in N_2 gas in order to attain cross-linking. The CLPE specimens were machined from this bar stock after cooling. The specimens were immersed in an acetone solution containing 10 mg/mL benzophenone for 30 s and then dried in the dark at room temperature to remove acetone. Using ultraviolet spectroscopy, the amount of benzophenone adsorbed on the surface was reported to be 3.5×10^{-11} mol/cm^2 in previous studies.[15,16] The MPC was dissolved in degassed pure water to attain concentrations ranging from 0.06 to 1.00 mol/L. Subsequently, the CLPE specimens coated with benzophenone were immersed in the aqueous MPC solutions. Photo-induced graft polymerization on the CLPE surface was performed using ultraviolet irradiation (UVL-400HA ultra-high pressure mercury lamp; Riko-Kagaku Sangyo, Funabashi, Japan) with an intensity of 5 mW/cm^2 at 60°C for 12–90 min; a filter (Model D-35; Toshiba, Tokyo, Japan) was used restrict the passage of ultraviolet light to wavelengths of 350 ± 50 nm. After polymerization, the CLPE-*g*-MPC specimens were removed, washed with pure water and ethanol, and dried at room temperature. These specimens were then sterilized by 25 kGy gamma-ray under N_2 gas.

Surface analysis by X-ray photoelectron spectroscopy, water-contact angle measurement, and Fourier-transform infrared spectroscopy

The surface elemental contents of CLPE-*g*-MPC obtained with various photo-irradiation times or MPC concentrations were analyzed using X-ray photoelectron spectroscopy (XPS). The XPS spectra were obtained using an XPS spectrophotometer (AXIS Hsi 165; Kratos Analytical, UK) equipped with an Mg-Kα radiation source by applying a voltage of 15 kV at the anode. The take-off angle of the photoelectrons was maintained at 90°. Each measurement was scanned five times, and five replicate measurements were performed on each sample, and the average values were considered for the surface elemental contents.

The static water-contact angles of CLPE-*g*-MPC obtained at various MPC concentrations were measured with an optical bench-type contact angle goniometer (Model DM300; Kyowa Interface Science, Saitama, Japan) using a sessile drop method. Drops of purified water (1 μL) were deposited on the CLPE-*g*-MPC surfaces, and the contact angles were directly measured after 60 s by using a microscope according to the ISO standard 15989.[29] Subsequently, 15 replicate measurements were performed on each sample, and the average values were taken as the contact angles.

The functional group vibrations of the CLPE-*g*-MPC surface that was polymerized with various MPC concentrations were examined using attenuated total reflection (ATR) by Fourier-transform infrared (FTIR) spectroscopy. FTIR/ATR spectra were obtained in 32 scans over a range of 800–2000 cm^{-1} by using an FTIR analyzer (FT/IR615; Jasco International, Tokyo, Japan) at a resolution of 4.0 cm^{-1}.

Cross-sectional observation of CLPE-*g*-MPC by transmission electron microscopy

A cross-section of the poly(MPC) layer on the CLPE-*g*-MPC surface produced at various MPC concentrations was observed using a transmission electron microscope (TEM). The specimens were first embedded in epoxy resin, stained with ruthenium oxide vapor at room temperature, and then sliced into ultra-thin films (approximately 100-nm thick) by using a Leica Ultra Cut UC microtome (Leica Microsystems, Wetzlar, Germany). A JEM-1010 electron microscope (JEOL, Tokyo, Japan) was used for the TEM observation at an acceleration voltage of 100 kV.

Surface coated-area observation by Fluorescence Microscopy (FM)

We used rhodamine 6G (Wako Pure Chemical Industries) because it can be easily and rapidly applied to a polymer coating and imaged using fluorescence microscopy (FM) (Axioskop 2 Plus; Carl Zeiss AG, Oberkochen, Germany). Wang et al. observed that rhodamine 6G effectively stains the MPC polymer, which shares very high structural similarity to lipids.[30]

An aqueous solution of 200 mass ppm rhodamine 6G was used for all the staining experiments. All the samples were stained using a two-step procedure. (1) The samples were immersed in the rhodamine 6G solution for 30 s and then removed. (2) Subsequently, they were washed twice consecutively in distilled water for 30 s and dried.

All the samples were examined and imaged using FM. Pseudo-color images were obtained using a charge-coupled-device (CCD) camera (VB-7010; Keyence, Osaka, Japan) and imaging software (VH analyzer 2.51; Keyence). Lenses with a 10× magnification and an appropriate exposure time (approximately 1/10 s) were employed to obtain clear images of the samples.

Friction test

The friction test was performed using a ball-on-plate machine (Tribostation 32; Shinto Scientific, Tokyo, Japan). Each of the CLPE-*g*-MPC surfaces with various MPC concentrations were used to prepare six sample pieces. A Co-Cr-Mo alloy ball with 9 mm in diameter was prepared. The surface roughness of the ball was Ra = 0.01, which was comparable with that of femoral ball products. The friction tests were performed at room temperature with a load of 0.98 N, sliding distance of 25 mm, and frequency of 1 Hz for a maximum of 100 cycles.[31] Pure water was used as a lubricant. The mean static (μ_s) and dynamic (μ_d) coefficients of friction were determined by averaging five data points from the 100 (96–100) cycle measurements.

Hip simulator wear test

A 12-station hip joint simulator (MTS Systems, MN, USA) with CLPE and CLPE-*g*-MPC cups both having an inner and outer diameter of 26 and 52 mm, respectively, was used for the hip simulator wear test. For each MPC concentration [0 (untreated), 0.25, and 0.50 mol/L], two sample pieces were prepared. A Co-Cr-Mo alloy femoral ball component with a size of 26 mm (Japan Medical Materials, Osaka, Japan) was used as the femoral component. A mixture of 25 vol % bovine serum, 20 m*M*/L of ethylene diamine tetraacetic acid (EDTA), and 0.1mass % sodium azide was used as a lubricant, according to the ISO standard 14242-1.[32] The lubricant was replaced every 0.5×10^6 cycles. Walks, which simulated a physiologic loading curve (Paul-type) with double peaks at 1793 and 2744 N loads, with a multidirectional (biaxial and orbital) motion of 1 Hz frequency were applied. Wear was determined by weighing the cups at intervals of 0.5×10^6 cycles. Load-soak controls ($n = 2$) were used to compensate the fluid absorption by the specimens.[33] The testing was continued until a total of 5.0×10^6 cycles were completed.

RESULTS

Figure 1 shows the phosphorous (P) concentration of the CLPE-*g*-MPC surface as a function of the photo-irradiation time during polymerization. The P concentration increased proportionally with the photo-irradiation time. When the photo-irradiation time was greater than 45 min, the P concentration of the CLPE-*g*-MPC surface with 0.17, 0.25, and 0.50 mol/L MPC concentration became almost constant at high values of 2.9, 3.8, and 4.6 atom %, respectively.

Figure 2 shows the nitrogen (N) and P content in the CLPE-*g*-MPC surface polymerized with various MPC concentrations and a 90-min photo-irradiation time. Both the N and P content in the CLPE-*g*-MPC surface increased to 5.2 up to an MPC concentration of 0.50 mol/L; it then gradually decreased with an

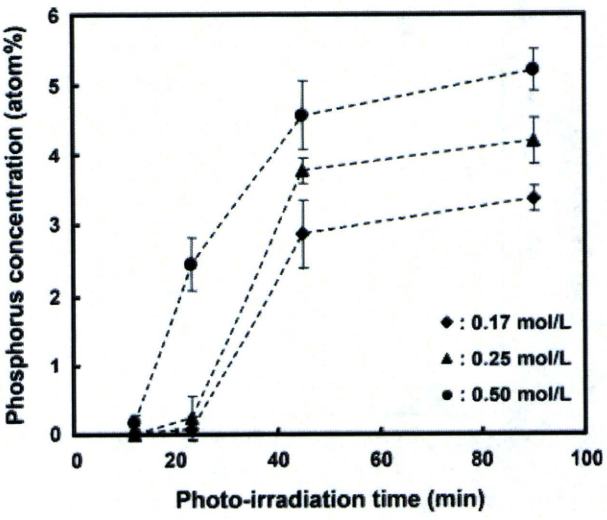

Figure 1. Phosphorus concentration in the CLPE-*g*-MPC surface as a function of the photo-irradiation time.

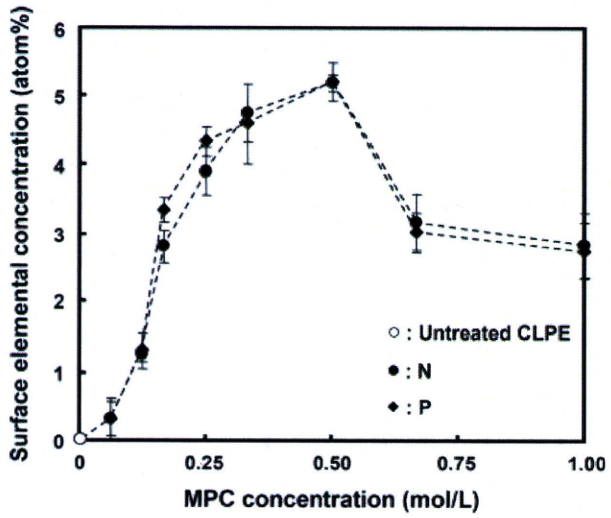

Figure 2. Surface elemental concentration of CLPE-*g*-MPC as a function of the MPC concentration with a 90-min photo-irradiation time.

increase in the MPC concentration. The N and P content at 0.50 mol/L MPC concentration was almost equivalent to the theoretical elemental composition (N = 5.3, P = 5.3) of poly(MPC).

Figure 3 shows the static water-contact angle of CLPE-*g*-MPC as a function of the MPC concentration used for polymerization (90-min photo-irradiation time). The static water-contact angle of untreated CLPE was 90° and decreased markedly with an increase in the MPC concentration during polymerization. When the MPC concentration was between 0.25 and 0.50 mol/L, the static water-contact angle was constant; the lowest value was recorded at 15°.

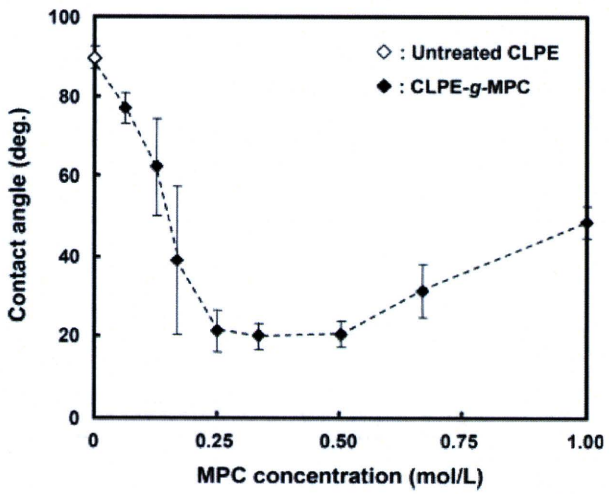

Figure 3. Static water-contact angle of CLPE-*g*-MPC as a function of the MPC concentration with a 90-min photo-irradiation time.

Figure 4 shows the FTIR/ATR spectra of untreated CLPE and CLPE-*g*-MPC obtained with various MPC concentrations and a 90-min photo-irradiation time. An absorption peak was observed at 1460 cm^{-1} for both CLPE and CLPE-*g*-MPC. This peak is chiefly attributed to the methylene (CH_2) chain in the CLPE substrate and the poly(MPC) chain. However, transmission absorption peaks at 1240, 1080, and 970 cm^{-1} were observed only for CLPE-*g*-MPC. These peaks corresponded to the phosphate group (P—O) in the MPC unit. Similarly, an absorption peak at 1720 cm^{-1} observed in CLPE-*g*-MPC corresponded only to the carbonyl group (C=O) in the MPC unit. The absorption peak intensity of the P—O group increased with the MPC concentration used for polymerization and reached its maximum at a concentration of 0.5 mol/L.

Figure 5 shows the cross-sectional TEM images of CLPE-*g*-MPC obtained with various MPC concentrations and a 90-min photo-irradiation time. At MPC concentrations greater than 0.25 mol/L, a 10–250-nm thick grafted poly(MPC) layer was clearly observed on the surface of the CLPE substrate. At an MPC concentration of 1.00 mol/L, the MPC-covered region coexisted with the uncovered regions, although the thickness of the poly(MPC) layer was greatest in the cover region, that is, 200–250 nm. At MPC concentrations below 0.06 mol/L, no poly(MPC) layer was observed on the CLPE surface (data not shown). These results indicate that the length of the grafted

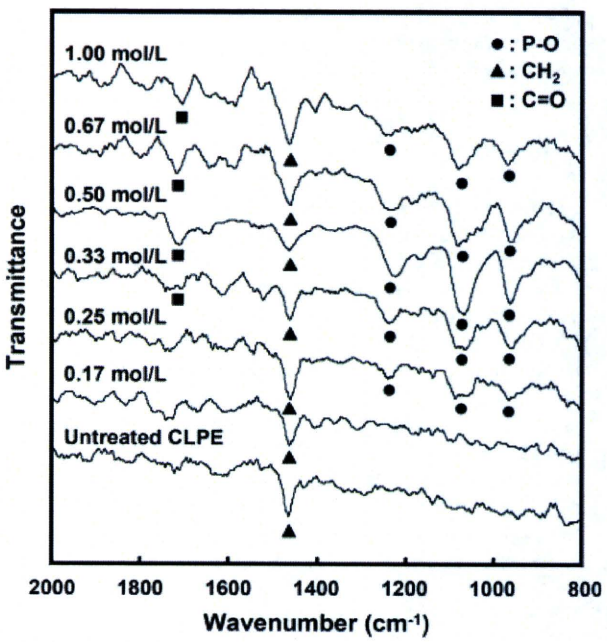

Figure 4. FT-IR/ATR spectra of CLPE-*g*-MPC obtained with various MPC concentrations and a 90-min photo-irradiation time.

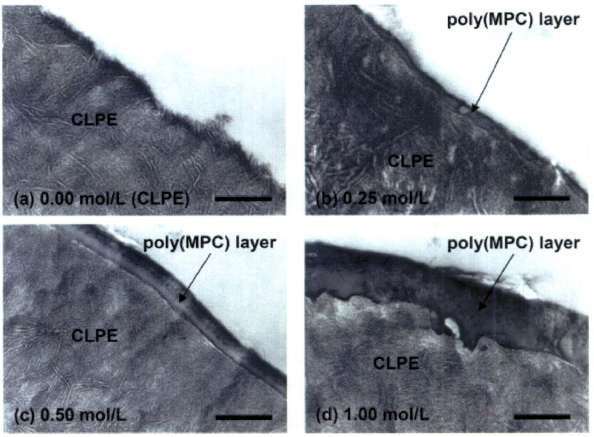

Figure 5. Cross-sectional TEM images of CLPE-*g*-MPC obtained with various MPC concentrations and a 90-min photo-irradiation time. Bar; 200 nm.

poly(MPC) chain (thickness of the poly(MPC) layer) can be controlled by adjusting the MPC concentration during polymerization. This is attributable to the fact that the length of the polymer chains produced in a radical polymerization reaction generally correlates with the MPC concentration.

Figure 6 shows the FM images of the CLPE-*g*-MPC surface with 0.50 and 1.00 mol/L MPC concentrations and a 90-min photo-irradiation time. The multiple lines observed on the FM images are machining marks. On the CLPE-*g*-MPC surface with an MPC concentration of 0.50 mol/L, the poly(MPC) layer stained with rhodamine 6G was clearly visible and showed uniform staining. On the CLPE-*g*-MPC surface with an MPC concentration of 1.00 mol/L, an ungrafted (unstained) region was observed, indicating nonuniform grafting of the poly(MPC) layer on the CLPE surface.

Figure 7 shows the static and dynamic coefficients of friction of CLPE-*g*-MPC obtained with various MPC concentrations and a 90-min photo-irradiation time. For CLPE-*g*-MPC, These coefficients of friction decreased markedly with an increase in MPC concentration and were the lowest at 0.5 and 0.25–0.5 mol/L, respectively; however, they increased at MPC concentrations above 0.67 mol/L. The CLPE-*g*-MPC specimens obtained with MPC concentrations of 0.25 and 0.50 mol/L exhibited ~80% reduction (i.e., 75–80%) in their dynamic coefficients of friction when compared with the untreated CLPE specimens.

Figure 8 shows the relationship between the dynamic coefficient of friction and the contact angle.

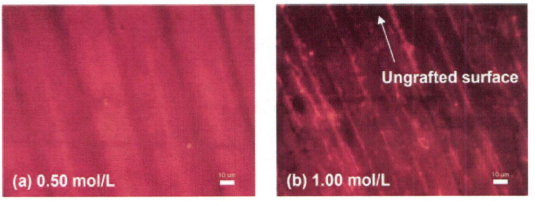

Figure 6. FM images of CLPE-*g*-MPC obtained with various MPC concentrations and a 90-min photo-irradiation time. Bar; 10 μm.

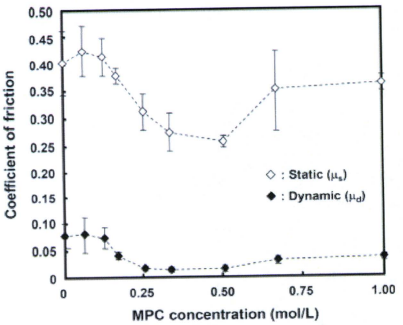

Figure 7. Coefficients of friction of the CLPE-*g*-MPC surface as a function of MPC concentration with a 90-min photo-irradiation time.

The dynamic coefficient of friction tended to increase with the contact angle. This increase was linear to a degree of accuracy, and the correlation coefficient was 0.920.

Figure 9 shows the gravimetric wear of the untreated CLPE and CLPE-*g*-MPC cups in the hip simulator wear test obtained with 0.25 and 0.50 mol/L MPC concentrations and a 90-min photo-irradiation time. It was observed that wear was significantly lower in the CLPE-*g*-MPC cups than in the untreated CLPE cups. There was no significant difference in wear of the CLPE-*g*-MPC cups obtained with 0.25 and 0.50 mol/L MPC concentrations. The CLPE-*g*-MPC

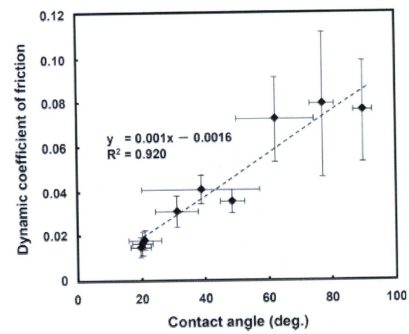

Figure 8. Relationship between dynamic coefficient of friction and contact angle in the CLPE-*g*-MPC surface. Bar; Standard deviations.

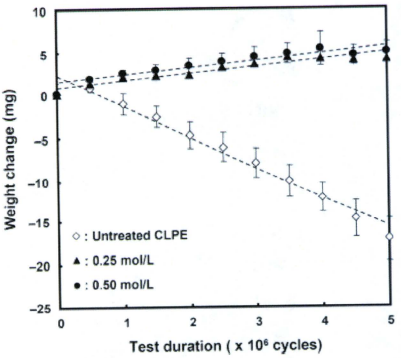

Figure 9. Weight change of the CLPE-*g*-MPC cups obtained with various MPC concentrations and a 90-min photo-irradiation in the hip joint simulator wear test. Bar; Standard deviations.

cups exhibited a slight increase in weight. This was partially attributable to enhanced fluid absorption in the tested cups than in the load-soak controls. When using the gravimetric method, the weight loss in the tested cups is corrected by subtracting the weight gain in the load-soak controls; however, this correction can not be perfectly achieved because only the tested cups are continuously subjected to motion and load. Fluid absorption in the tested cups is generally slightly higher than that in the load-soak controls. Consequently, the correction for fluid absorption by using the load-soak data as the correction factor leads to a slight underestimation of the actual weight loss.[12,33] In this study, a steady wear rate was calculated using data from 4.0×10^6 to 5.0×10^6 cycles; this value was 5.11 mg/10^6 cycles in the untreated CLPE cups. In contrast, the wear rates of the CLPE-*g*-MPC cups with 0.25 and 0.50 mol/L MPC concentrations were markedly lower, that is, 0.12 and 0.32 mg/10^6 cycles, respectively.

DISCUSSION

In this study, we investigated the properties of the poly(MPC) layer formed on the CLPE surface with various MPC concentrations by using photo-induced radical graft polymerization. The wear resistant properties of CLPE-*g*-MPC in terms of the characteristics of the nanometer-scale layer of poly(MPC) will be discussed hereafter.

In Figure 2, both the N and P content in the CLPE-*g*-MPC surface attributed to poly(MPC) increased to

5.2 with an increase in the MPC concentration during polymerization. In addition, in the TEM images shown in Figure 5, the thickness of the poly(MPC) layer increased with the MPC concentration. When the poly(MPC) layer has a brush-like structure, the layer thickness may correlate with the molecular weight of the grafted poly(MPC). The high-density poly(MPC) graft chains in the CLPE-g-MPC, are assumed to exhibit a brush-like structure.[34,35] It is generally well known that the reaction rate of radical polymerization is extremely high.[36] In this study, the length (molecular weight) of the poly(MPC) graft chains was assumed to be successfully controlled by the MPC concentration used for polymerization. This indicates that the length of the poly(MPC) chain grafted on the CLPE surface increased with the MPC concentration during polymerization.[37] The molecular weight of the grafted poly(MPC) chain on the CLPE-g-MPC surface could not be determined due to the difficulty in separating the grafted poly(MPC) chain from the CLPE substrate. Additional efforts are needed in this aspect.

In the TEM observation, the thickest poly(MPC) layer (200–250 nm) was observed on the CLPE-g-MPC surface with a 1.00 mol/L MPC concentration [Fig. 5(d)]. However, the N and P content in the CLPE-g-MPC surface decreased at MPC concentrations above 0.67 mol/L (Fig. 2). On the CLPE-g-MPC surface with a 1.00 mol/L MPC concentration, an ungrafted (unstained) CLPE region was observed in the FM image [Fig. 6(b)]. The present graft polymerization reaction with free radicals is photo-induced by ultraviolet-ray irradiation using benzophenone as a radical initiator. On the contrary, a certain amount of ultraviolet-ray irradiation energy can directly produce free radicals form the methacryl acid group of the MPC unit in the monomer solution. When the MPC concentration in a feed is high, graft polymerization between the radicals on the CLPE surface and the MPC monomer and homopolymerization of MPC occurs simultaneously in the reaction system. The free radicals not only facilitate direct grafting of MPC to CLPE, thereby forming C—C covalent bonds between the MPC polymer and the CLPE substrate, but also induce homopolymerization of MPC as a free polymer in the solution. Moreover, the diffusion of the monomer might be interfered in the polymer solution with high concentration because of high viscosity. When the monomer and initiator attached to the CLPE surface were subjected to ultraviolet-ray irradiation, radicals were freely formed on the CLPE surface in the early stage but not in the late stage of polymerization, probably because the increased polymer radicals and/or grown grafted polymer chains blocked the diffusion of the radicals to the CLPE surface.[38] Therefore, it is supposed that the ungrafted bare CLPE surface appeared due to a decrease in the MPC concentration during graft polymerization and homopolymerization.

When the photo-irradiation time was fixed (90 min in the present study), the grafting efficiency (N and P content) of the CLPE-g-MPC surface increased with the MPC concentration up to 0.50 mol/L and then decreased at concentration above 0.67 mol/L. It is assumed that when the monomer concentrations in a feed is low (0–0.50 mol/L), the rate of MPC homopolymerization is higher than that of MPC graft polymerization. In contrast, when the monomer concentrations in a feed is high (>0.67 mol/L), the rate of MPC graft polymerization might be higher than that of MPC homopolymerization. Moreover, while the rate of MPC graft polymerization increases with the MPC concentration, the entire polymerization system begins to show gelation at MPC concentrations above 0.67 mol/L and the grafting efficiency might drastically decrease. In Figure 1, when the photo-irradiation time was greater than 45 min, the P concentration in CLPE-g-MPC became constant at high values for all the MPC concentrations. It has been reported that the photo-irradiation time must be controlled to obtain a high-density poly(MPC) layer.[12] The density of the poly(MPC) chains on the CLPE surface gradually increased with the photo-irradiation time and the entire CLPE surface was grafted with a photo-irradiation time greater than 45 min (approximately 90 min in the present study). From the above results, it is clear that to achieve high grafting efficiency for CLPE-g-MPC, it is essential to use a long photo-irradiation time in the polymerization system, which contains a high-concentration monomer without gelation.

In our previous studies, the mechanism of wear reduction has been reported.[10–13] Since MPC is a highly hydrophilic compound, poly(MPC) is water-soluble. The water-wettability of the CLPE-g-MPC surface is considerably greater than that of the untreated CLPE surface. Kobayashi et al. reported that the water molecules adsorbed on the surface of the highly hydrophilic poly(MPC) brushes act as a lubricants and reduce the interaction between the brushes and the counter-bearing face.[39] Therefore, the artificial hip joint bearing with the grafted poly(MPC) surface exhibits considerably greater lubricity than that without the poly(MPC) surface. In Figure 8, we observed that water-wettability (static water-contact angle) corresponded with the dynamic coefficient of friction. The significant reduction in the coefficient of friction of the grafted poly(MPC) surface resulted in a substantial improvement in wear resistance.[10,40] Fluid-film lubrication (or mixed lubrication) of the artificial hip joint bearing with the grafted poly(MPC) surface was achieved by the intermediate hydrated layer. It can be affirmed that this novel artificial hip joint utilizing poly(MPC) mimics the natural joint cartilage. The fluid (water)-film forming ability of a

10-nm-thick poly(MPC) layer is equivalent to that of a micrometer-order-thick poly(MPC) layer because the outermost poly(MPC) layer determines this ability. The hip joint simulator wear test confirmed that the wear rate was much lower in the CLPE-*g*-MPC cups than in the untreated CLPE cups (Fig. 9). The water-wettability of the CLPE-*g*-MPC surface was greater than that of the untreated CLPE surface because of the presence of a poly(MPC) nanometer-scale layer. At an MPC concentration of 0.25 mol/L, the orthopaedic bearing with the CLPE-*g*-MPC surface exhibited high lubricity because the poly(MPC) layer supported a thin film of water on its surface even at a thickness of 10 nm. Consequently, the 10-nm-thick poly(MPC) layer was responsible for the improved wear resistance, which is independent of its thickness. When the CLPE surface is modified by poly(MPC) grafting, the MPC graft polymer causes a significant reduction in sliding friction between the graft surfaces because the water thin films that are formed act as extremely efficient lubricants. The water-lubrication systems utilizing poly(MPC) suppress direct contact of the counter-bearing face with the CLPE substrate in order to reduce the frictional force.[39,41] Thus nanometer-scale modifications of CLPE with poly(MPC) is expected to significantly increase the durability of the orthopaedic bearings. Poly(MPC) grafting obtained with an MPC concentration of 0.50 mol/L is particularly effective in maintaining the wear resistance of CLPE-g-MPC for use as an orthopedic bearing material over a long time periods.[11]

CONCLUSION

The effect of MPC concentration on photo-induced radical graft polymerization was examined, and the resultant properties of CLPE-*g*-MPC were discussed with respect to the characteristics of the poly(MPC) nanometer-scale layer. The thickness of the grafted poly(MPC) layer increased with the MPC concentration in the feed. The hip joint simulator wear test confirmed that the wear rate of the CLPE-*g*-MPC cups was considerably lower than that of the untreated CLPE cups. Since MPC is a highly hydrophilic compound, the water-wettability of the CLPE-*g*-MPC surface was greater than that of the untreated CLPE surface due to the formation of a poly(MPC) nanometer-scale layer. The CLPE-*g*-MPC orthopaedic bearing surface exhibited high lubricity by poly(MPC) layer even 10-nm thick. This layer is considered responsible for the improved wear resistance. Nanometer-scale modification of CLPE with poly(MPC) is expected to significantly increase the durability of the orthopaedic bearings. It is necessary to use a long photo-irradiation time in the polymerization system, which contains a high-concentration monomer without gelation, to attain such a nanometer scale modification with poly(MPC).

We express special thanks to Mr. Yoshiki Ando, Mr. Makoto Kondo, Mr. Takatoshi Miyashita, and Mr. Noboru Yamawaki (Japan Medical Materials, Osaka, Japan) for their excellent technical assistance.

References

1. Iwasaki Y, Ishihara K. Phosphorylcholine-containing polymers for biomedical applications. Anal Bioanal Chem 2005; 381:534–546.
2. Binyamin G, Shafi BM, Mery CM. Biomaterials: A primer for surgeons. Semin Pediatr Surg 2006;15:276–283.
3. Kurtz S, Mowat F, Ong K, Chan N, Lau E, Halpern M. Prevalence of primary and revision total hip and knee arthroplasty in the United States from 1990 through 2002. J Bone Joint Surg Am 2005;87:1487–1497.
4. Harris WH. The problem is osteolysis. Clin Orthop Relat Res 1995;311:46–53.
5. Sochart DH. Relationship of acetabular wear to osteolysis and loosening in total hip arthroplasty. Clin Orthop Relat Res 1999;363:135–150.
6. Oonishi H, Clarke IC, Good V, Amino H, Ueno M. Alumina hip joints characterized by run-in wear and steady-state wear to 14 million cycles in hip-simulator model. J Biomed Mater Res A 2004;70:523–532.
7. McMinn DJ, Daniel J, Pynsent PB, Pradhan C. Mini-incision resurfacing arthroplasty of hip through the posterior approach. Clin Orthop Relat Res 2005;441:91–98.
8. Muratoglu OK, Bragdon CR, O'Connor DO, Jasty M, Harris WH. A novel method of cross-linking ultra-high-molecular-weight polyethylene to improve wear, reduce oxidation, and retain mechanical properties. Recipient of the 1999 HAP Paul Award. J Arthroplasty 2001;16:149–160.
9. Kyomoto M, Iwasaki Y, Moro T, Konno T, Miyaji F, Kawaguchi H, Takatori Y, Nakamura K, Ishihara K. High lubricious surface of cobalt-chromium-molybdenum alloy prepared by grafting poly(2-methacryloyloxyethyl phosphorylcholine). Biomaterials 2007;28:3121–3130.
10. Moro T, Takatori Y, Ishihara K, Konno T, Takigawa Y, Matsushita T, Chung UI, Nakamura K, Kawaguchi H. Surface grafting of artificial joints with a biocompatible polymer for preventing periprosthetic osteolysis. Nat Mater 2004;3:829–837.
11. Moro T, Takatori Y, Ishihara K, Nakamura K, Kawaguchi H. 2006 Frank Stinchfield Award: Grafting of biocompatible polymer for longevity of artificial hip joints. Clin Orthop Relat Res 2006;453:58–63.
12. Kyomoto M, Moro T, Konno T, Takadama H, Yamawaki N, Kawaguchi H, Takatori Y, Nakamura K, Ishihara K. Enhanced wear resistance of modified cross-linked polyethylene by grafting with poly(2-methacryloyloxyethyl phosphorylcholine). J Biomed Mater Res A 2007;82:10–17.
13. Kyomoto M, Moro T, Konno T, Takadama H, Kawaguchi H, Takatori Y, Nakamura K, Yamawaki N, Ishihara K. Effects of photo-induced graft polymerization of 2-methacryloyloxyethyl phosphorylcholine on physical properties of cross-linked polyethylene in artificial hip joints. J Mater Sci Mater Med 2007;18:1809–1815.
14. Ishihara K, Ueda T, Nakabayashi N. Preparation of phospholipid polymers and their properties as polymer hydrogel membranes. Polym J 1990;22:355–360.
15. Ishihara K, Iwasaki Y, Ebihara S, Shindo Y, Nakabayashi N. Photoinduced graft polymerization of 2-methacryloyloxyethyl

phosphorylcholine on polyethylene membrane surface for obtaining blood cell adhesion resistance. Colloids Surf B Biointerfaces 2000;18:325–335.
16. Sibarani J, Takai M, Ishihara K. Surface modification on microfluidic devices with 2-methacryloyloxyethyl phosphorylcholine polymers for reducing unfavorable protein adsorption. Colloids Surf B Biointerfaces 2007;54:88–93.
17. Ueda H, Watanabe J, Konno T, Takai M, Saito A, Ishihara K. Asymmetrically functional surface properties on biocompatible phospholipid polymer membrane for bioartificial kidney. J Biomed Mater Res A 2006;77:19–27.
18. Abraham S, Brahim S, Ishihara K, Guiseppi-Elie A. Molecularly engineered p(HEMA)-based hydrogels for implant biochip biocompatibility. Biomaterials 2005;26:4767–4778.
19. Konno T, Hasuda H, Ishihara K, Ito Y. Photo-immobilization of a phospholipid polymer for surface modification. Biomaterials 2005;26:1381–1388.
20. Palmer RR, Lewis AL, Kirkwood LC, Rose SF, Lloyd AW, Vick TA, Stratford PW. Biological evaluation and drug delivery application of cationically modified phospholipid polymers. Biomaterials 2004;25:4785–4796.
21. Snyder TA, Tsukui H, Kihara S, Akimoto T, Litwak KN, Kameneva MV, Yamazaki K, Wagner WR. Preclinical biocompatibility assessment of the EVAHEART ventricular assist device: Coating comparison and platelet activation. J Biomed Mater Res A 2007;81:85–92.
22. Kuiper KK, Nordrehaug JE. Early mobilization after protamine reversal of heparin following implantation of phosphorylcholine-coated stents in totally occluded coronary arteries. Am J Cardiol 2000;85:698–702.
23. Ho SP, Nakabayashi N, Iwasaki Y, Boland T, LaBerge M. Frictional properties of poly(MPC-*co*-BMA) phospholipid polymer for catheter applications. Biomaterials 2003;24:5121–5129.
24. Lewis AL, Hughes PD, Kirkwood LC, Leppard SW, Redman RP, Tolhurst LA, Stratford PW. Synthesis and characterisation of phosphorylcholine-based polymers useful for coating blood filtration devices. Biomaterials 2000;21:1847–1859.
25. Pavoor PV, Gearing BP, Muratoglu O, Cohen RE, Bellare A. Wear reduction of orthopaedic bearing surfaces using polyelectrolyte multilayer nanocoatings. Biomaterials 2006;27:1527–1533.
26. Yamamoto M, Kato K, Ikada Y. Ultrastructure of the interface between cultured osteoblasts and surface-modified polymer substrates. J Biomed Mater Res 1997;37:29–36.
27. Wang P, Tan KL, Kang ET. Surface modification of poly(tetrafluoroethylene) films via grafting of poly(ethylene glycol) for reduction in protein adsorption. J Biomater Sci Polym Ed 2000;11:169–186.
28. Iwata R, Suk-In P, Hoven VP, Takahara A, Akiyoshi K, Iwasaki Y. Control of nanobiointerfaces generated from well-defined biomimetic polymer brushes for protein and cell manipulations. Biomacromolecules 2004;5:2308–2314.
29. ISO. Plastics–Film and sheeting–Measurement of water-contact angle of corona-treated films. International Organization for Standardization 15989, 2004.
30. Wang JH, Bartlett JD, Dunn AC, Small S, Willis SL, Driver MJ, Lewis AL. The use of rhodamine 6G and fluorescence microscopy in the evaluation of phospholipid-based polymeric biomaterials. J Microsc 2005;217 (Part 3):216–224.
31. ASTM F732-00: Standard test method for wear testing of polymeric materials used in total joint prostheses. In: Annual Book of ASTM Standards 13. West Conshohocken: ASTM; 2004.
32. ISO. Implants for surgery: Wear of total hip-joint prostheses Part 1: Loading and displacement parameters for wear-testing machines and corresponding environmental conditions for test. 2002. International Organization for Standardization 14242-1.
33. ISO. Implants for surgery: Wear of total hip-joint prostheses, Part 2: Methods of measurement. 2000. International Organization for Standardization 14242-2.
34. Matsuda T, Kaneko M, Ge S. Quasi-living surface graft polymerization with phosphorylcholine group(s) at the terminal end. Biomaterials 2003;24:4507–4515.
35. Goda T, Konno T, Takai M, Moro T, Ishihara K. Biomimetic phosphorylcholine polymer grafting from polydimethylsiloxane surface using photo-induced polymerization. Biomaterials 2006;27:5151–5160.
36. Braunecker WA, Matyjaszewski K. Controlled/living radical polymerization: Features, developments, and perspectives. Prog Polym Sci 2007;32:93–146.
37. Ma H, Davis RH, Bowman CN. A novel sequential photoinduced living graft polymerization. Macromolecules 2000;33:331–335.
38. Hegazy EA, Dessouki AM, El-Dessouky MM, El-Sawy NM, Crosslinked grafted PVC obtained by direct radiation grafting. Radiat Phys Chem 1985;26:143–149.
39. Kobayashi M, Terayama Y, Hosaka N, Kaido M, Suzuki A, Yamada N, Torikai N, Ishihara K, Takahara A. Friction behavior of high-density poly(2-methacryloyloxyethyl phosphorylcholine) brush in aqueous media. Soft Matter 2007;2:740–746.
40. Goda T, Konno T, Takai M, Ishihara K. Photoinduced phospholipid polymer grafting on Parylene film: Advanced lubrication and antibiofouling properties. Colloids Surf B Biointerfaces 2007;54:67–73.
41. Raviv U, Glasson S, Kampf N, Gohy JF, Jérôme R, Klein J. Lubrication by charged polymers. Nature 2003;425:163–165.

Available online at www.sciencedirect.com
ScienceDirect
Biomaterials 29 (2008) 1367–1376
Biomaterials
www.elsevier.com/locate/biomaterials

Surface tethering of phosphorylcholine groups onto poly(dimethylsiloxane) through swelling–deswelling methods with phospholipids moiety containing ABA-type block copolymers

Ji-Hun Seo, Ryosuke Matsuno, Tomohiro Konno, Madoka Takai, Kazuhiko Ishihara*

Department of Materials Engineering, School of Engineering and Center for NanoBio Integration, The University of Tokyo, 7-3-1 Hongo, Bunkyo-ku, Tokyo 113-8656, Japan

Received 29 August 2007; accepted 24 November 2007
Available online 26 December 2007

Abstract

The surface modification of poly(dimethylsiloxane) (PDMS) substrates by using ABA-type block copolymers comprising poly(2-methacryloyloxyethyl phosphorylcholine (MPC)) (PMPC) and PDMS segments was investigated. The hydrophobic interaction between the swelling–deswelling nature of PDMS and PDMS segments in block copolymers was the main mechanism for surface modification. Block copolymers with various compositions were synthesized by using the atom transfer radical polymerization (ATRP) method. The kinetic plots revealed that polymerization could be initiated by PDMS macroinitiators and it proceeds in a well-controlled manner; therefore, the compositions of the block copolymers were controllable. The obtained block copolymers were dissolved in a chloroform/ethanol mixed solvent. The surface of the PDMS substrate was modified using block copolymers by the swelling–deswelling method. Static contact angle and X-ray photoelectron spectroscopy (XPS) measurements revealed that the hydrophobic surface of the PDMS substrate was converted to a hydrophilic surface because of modification by surface-tethered PMPC segments. Protein adsorption test and L929 cell adhesion test were carried out for evaluating the biocompatibility. As observed, the amount of adsorbed proteins and cell adhesion were drastically reduced as compared to those in the non-treated PDMS substrate. We conclude that this procedure is effective in fabricating biocompatible surfaces on PDMS substrates.

Keywords: 2-Methacryloyloxyethyl phosphorylcholine; Poly(dimethylsiloxane); Atom transfer radical polymerization; Biocompatibility; Swelling–deswelling method

1. Introduction

Polydimethylsiloxane (PDMS) has many attractive engineering properties such as high oxygen permeability, good formability, chemical stability, optical transparency, and good mechanical properties. Because of these reasons, PDMS has been used in many engineering fields employing biomaterials, such as making artificial organs, and recently as a base material for manufacturing biochips [1–3]. However, due to the hydrophobic nature of its surface, biological components found in blood and body fluids interact strongly with the PDMS surface when it is present in a biological environment. A significant amount of protein adsorption onto the PDMS surface caused by such a hydrophobic interaction is the most important problem to be overcome because it triggers many undesirable bioreactions [4,5]. Therefore, in order to construct a biofunctional surface to prevent the nonspecific adsorption of proteins is essential for the proper functioning of PDMS-based biomaterials.

When modifying the surface, selecting biocompatible materials and the modifying method should be firstly considered. As biocompatible materials, poly(2-hydroxyethyl methacrylate), poly(ethylene glycol) (PEG), poly(acrylic acid), and 2-methacryloyloxyethyl phosphorylcholine (MPC) polymers

* Corresponding author. Department of Materials Engineering, School of Engineering, The University of Tokyo, 7-3-1 Hongo, Bunkyo-ku, Tokyo 113-8656, Japan. Tel.: +81 3 5841 7124; fax: +81 3 5841 8647.
E-mail address: ishihara@mpc.t.u-tokyo.ac.jp (K. Ishihara).

0142-9612/$ - see front matter © 2007 Elsevier Ltd. All rights reserved.
doi:10.1016/j.biomaterials.2007.11.039

have been researched as modifying materials [6–9]. Among these, MPC has been known to be a long-term biocompatible material and very easily applicable because of the large number of free water fractions around the zwitterionic phosphorylcholine head groups and its methacrylate backbone [9–16].

Chemical techniques to modify PDMS by using MPC as a biocompatible material have been researched for last decade. Xu et al. [17] fabricated PMPC segments onto silicone films by means of an ozone-induced grafting method, these segments exhibited good blood compatibility. Goda et al. [9] successfully introduced PMPC chains onto PDMS surfaces by means of UV-induced grafting using benzophenone as the initiator. They revealed non-biofouling PDMS surfaces and a reduction in the friction coefficient. Iwasaki et al. [18] used the ABA-type triblock copolymers composed of PMPC segments as an A-block and poly(vinylmethyl siloxane-co-dimethylsiloxane) as a B-block. The hydrosilyl-group-functionalized PDMS film surface was successfully reacted with the B-block and could form a lower biofouling surface. Although these chemical techniques are clearly powerful tools to modify the PDMS surface, they still have several disadvantages such as complexity in processing, the possibility of side reactions, chemical contamination (e.g., remaining initiators), and the dependence of the PDMS shapes. Physical techniques are relatively free from such problems. Commonly used physical techniques for modifying the surface of silicone-based materials are usually carried out by using plasma treatments or the deposition of modifying materials [19]. One of the simplest physical techniques recently developed is the swelling–deswelling method that uses a block copolymer comprising PDMS segments [20]. In this study, this relatively simple methodology of surface modification (as compared to both chemical and commonly used physical techniques) was applied to construct a hydrophilic PDMS material. We introduce an anti-biofouling PDMS surface by using a very simple swelling–deswelling method with ABA-type block copolymers comprising PMPC and PDMS segments. A MPC polymer was used to inhibit both protein and cell adhesion, which was partially difficult when PEG was used [21]. In order to investigate the effect of molecular weight on the surface characteristics, all the block copolymers were synthesized by means of the atom transfer radical polymerization (ATRP) method because of its broad utility in synthesizing block copolymers by using very different types of two or more species such as PMPC and PDMS [22–24]. The biocompatibility of the PDMS substrate modified by means of the swelling–deswelling method was tested by investigating the amount of adsorbed proteins and the cell adhesion test.

2. Materials and methods

2.1. Materials

MPC was synthesized as previously described [25]. Hydrosilyl-terminated poly(dimethylsiloxane) (Mn = 1014) was purchased from Gelest (Morrisville, PA, USA). Further, 2,2′-bipyridyl was obtained from Kanto Chemical (Tokyo, Japan); the solvent used in this study was purchased from Wako Chemical (Osaka, Japan) and used as received. Allyl 2-bromoisobutyrate, Cu(I)Cl, 2-methyl-1,4-naphthoquinon, and Karstedt's catalyst were purchased from Sigma–Aldrich (St. Louis, MO, USA). A Sylgard 184 silicone elastomer kit was purchased from Dow Corning (Midland, MI, USA). Dulbecco's phosphate-buffered saline (10×) (PBS: without calcium chloride and magnesium chloride) was purchased from Invitrogen Corporation (Carlsbad, CA, USA). Bovine plasma fibrinogen (BPF: F-8630) and bovine serum albumin (BSA: A-8022) were obtained from Sigma Chemical Co. (St. Louis, MO, USA). A micro-BCA protein assay reagent kit (#23235) was purchased from Pierce Chemical (Rockford, IL, USA).

The PDMS substrate was prepared as follows: a mixture of the PDMS precursor and cross-linker (10:1 by mass) (Toray Dow Corning, Tokyo, Japan) was spread on a Petri dish and cured in a vacuum oven at 70 °C for a day after degassing. Then, the sample was cut into quadrangles (10 × 10 × 2 mm).

2.2. Synthesis of ABA block copolymer

The PDMS macroinitiator was synthesized by means of a previously reported method [23]. A typical polymerization process could be described as follows: 0.332 g (0.232 mmol of the overall molecular weight) of the synthesized PDMS macroinitiator was placed into a 20 mL flask with 2.5 g MPC (8.5 mmol) and 5 mL methanol. The solution was bubbled with Ar gas for 15 min. Then, a mixture of 0.046 g (0.46 mmol) of Cu(I)Cl and 0.145 g (0.928 mmol) of 2,2′-bipyidyl was put into the flask and sealed using a rubber septum. A syringe-capped Ar balloon was placed at the septum, and the mixture was stirred at room temperature until a homogeneous maroon solution was formed. Periodically, 0.1 mL aliquots of the reaction mixture were removed for the kinetic analysis. After the reaction, 10 mL of methanol was poured into the mixture and then filtered through an alumina column to remove the transition metal catalyst. A clear colorless reaction mixture was then reprecipitated in a large amount of ether and chloroform (7:3) mixed solvent followed by a dialysis process for a day. After freeze-drying, a white block copolymer was obtained. Four different polymer compositions were synthesized by controlling the reaction time.

2.3. Swelling–deswelling of PDMS

The solvent composition suitable for the substrate was determined by investigating the swelling ratio of the PDMS substrate and the solubility of the block copolymers in six compositions of chloroform/ethanol mixed solvents. The PDMS substrate was immersed into a mixed solvent whose chloroform compositions were 100, 90, 70, 50, 30, and 0 vol% for a day at room temperature. After confirming if the swelling state reached the equilibrium state, the swelling ratio was calculated as follows:

$$\text{Swelling ratio}(\%) = \frac{(W_s - W_d)}{W_d} \times 100$$

where W_s and W_d denote the swelled and deswelled weights, respectively.

The synthesized block copolymers were dissolved in 70 vol% chloroform mixed solvent at 10 mg/mL and 30 mg/mL. Further, the PDMS substrates were immersed into 1 mL of each polymer solution for 5 days at room temperature. After rinsing by a fresh mixed solvent, the samples were dried in a vacuum oven at 60 °C for 6 h, followed by performing the first contact angle measurement. The samples were then aged in 5 mL of water at room temperature for 3 days, followed by thorough rinsing with water and drying in a vacuum oven for a day; then the second contact angle measurement was performed.

2.4. Characterization

2.4.1. ATRP characterization

The monomer conversion was calculated by comparing the NMR peak integrals due to the groups in the MPC monomer at $\delta = 5.5$ and $\delta = 6.0$ with those of the α-methyl group in the polymer chain at $\delta = 0.5$–1.1. The size exclusion chromatography (SEC) measurement was conducted using a JASCO RI-1530 detector containing two connected gel columns (TSK-GEL Super HM-M) with a poly(methyl methacrylate) standard in hexafluoroisopropanol (flow rate: 0.2 mL/min at 40 °C).

2.4.2. Contact angle measurement in water

The static water contact angles were measured by using a goniometer (Kyowa Interface Science Co., Tokyo, Japan) at room temperature. All the samples were dried in a vacuum oven for a day before the measurement. Then, water droplets of 3 μL were contacted with the samples for 5 s and the contact angles were measured using photographic images. More than three positions were measured for each sample.

2.4.3. X-ray photoelectron spectroscopy (XPS) measurement

The surface-tethered materials were investigated by XPS using magnesium K_α sources with a take-off angle of 90° (Kratos/Shimadzu, Kanagawa, Japan). All the samples were vacuum dried at 60 °C for a day before the measurement. The characterized elements were C, O, N, and P, and the binding energies were referenced to the C1s peak at 285.0 eV.

2.4.4. Atomic force microscope (AFM) observation

The AFM images under the wet condition were analyzed using NanoScope IIIa (Nihon Veeco, Tokyo, Japan). The excitation frequency range was 7.8–9 kHz, and the scan rate and scan scales were 0.5 Hz and 50 nm, respectively. All the samples were aged in water for a day before the observation and the scanning size of all the samples was 25 μm × 25 μm each.

2.5. Biocompatibility evaluation

2.5.1. Protein adsorption test

All the samples were aged in water for 3 days in order to remove the physically adsorbed block copolymers and ensure the existence of the tethered block copolymers. The PDMS substrates were immersed in a mixture of 0.03 g/dL BPF and 0.045 g/dL BSA in PBS (pH 7.4 and ion strength of 0.15 M) for 60 min at 37 °C and then rinsed with 500 mL of fresh PBS twice by the stirring method (300 rpm for 5 min). The adsorbed protein was detached in sodium dodecyl sulfate (SDS) (1 wt% in water) by sonication for 20 min, and the protein concentration in the SDS solution was determined by using the micro-BCA method [26]. By using the concentration of the standard protein solution, the amount of adsorbed proteins was calculated.

2.5.2. L929 cell adhesion test

The adhesion test of L929 fibroblasts (RCB 0081, Cell Bank, Japan) onto the modified PDMS substrate was carried out. The cells were grown with each PDMS substrate in 1 mL of the minimum essential medium (Gibco BRL Life Technologies, Eragny, France), supplemented by 10% fetal bovine serum (FBS) and penicillin (50 μg/mL). All the samples were stored in a 100% humidified incubator at 37 °C with 5% CO_2 for a day. After washing with fresh medium, all the PDMS substrates were observed using an optical microscope (Olympus Optical Co. LTD. IX71S1F-2, Tokyo, Japan).

3. Results and discussion

3.1. Synthesis of ABA block copolymer

Well-defined block-type copolymers comprising MPC units have been synthesized by photoinduced living radical polymerization and the reversible addition-fragmentation chain transition polymerization of MPC and other methacrylates [27,28]. In this study, we applied the ATRP of MPC from the macroinitiators of PDMS to develop PDMS/PMPC block copolymers because of the large difference in solubility between PDMS and PMPC (Scheme 1). Fig. 1 shows the kinetic plot of ln ($[M]_0/[M]$) versus reaction time for the ATRP of PDMS macroinitiators with MPC monomers. The resulting first-order slope indicates that the polymerization reactions proceeded with an approximately constant number of active species for the duration of the reaction; therefore, it was assumed that the contribution of the termination reactions could be neglected even under the limited solubility condition of the PDMS macroinitiators.

Fig. 2 shows the molecular weight evolution Mn and PDI as a function of the monomer conversion. As indicated in Eq. (1),

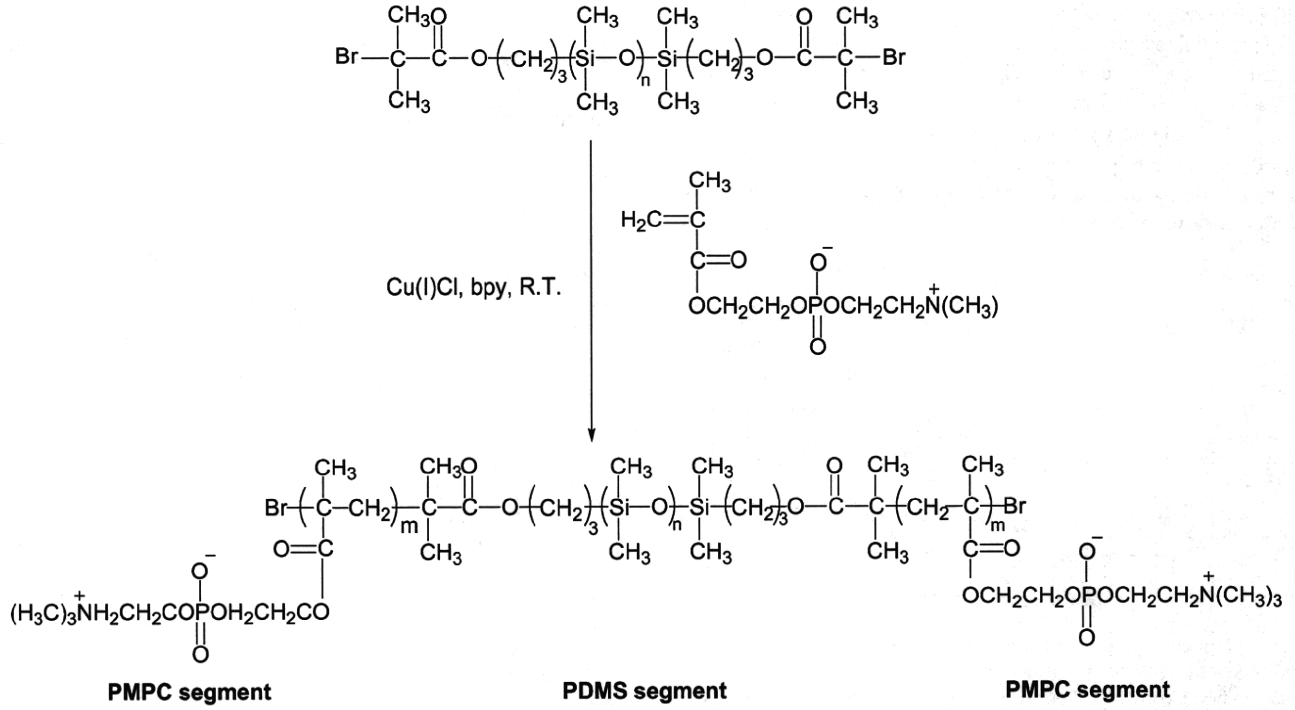

Scheme 1. Reaction scheme and molecular structure of ABA triblock copolymer.

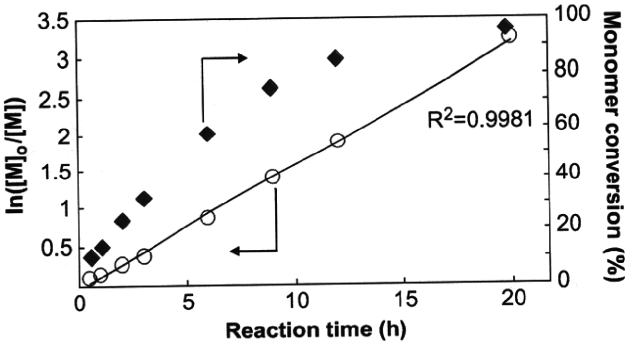

Fig. 1. Kinetic plot for the ATRP of MPC by PDMS macroinitiators to form the PDMS/PMPC block copolymer.

a linear increase in Mn versus monomer conversion was observed.

$$Mn_{theory} = Mn_{macroinitiator} + \frac{[Mn]_{monomer}}{[Mn]_{macroinitiator}} Mn_{monomer} \times \text{Conversion} \quad (1)$$

However, the molecular weights measured by SEC were much larger than those calculated using Eq. (1). This is caused by the difference between the number of calculated and synthesized PDMS macroinitiators. Since the final product of the PDMS macroinitiators was assumed to be 100% of the synthesized macroinitiators, the molecular weight of the synthesized polymer with a conversion of 96% should be approximately 10 kDa. On the basis of this calculation, the actual end functionality of the PDMS macroinitiators was approximately 20%, this was the reason why the overall molecular weight of the synthesized polymer was five times larger than the calculated value. These relatively low-end functionalities (10–55%) of the PDMS macroinitiators synthesized using allyl 2-bromoisobutyrate was already reported [23]. All the polymers used in this study were synthesized considering this result: a molecular weight that is five times greater than the infeed compositions of MPC was targeted.

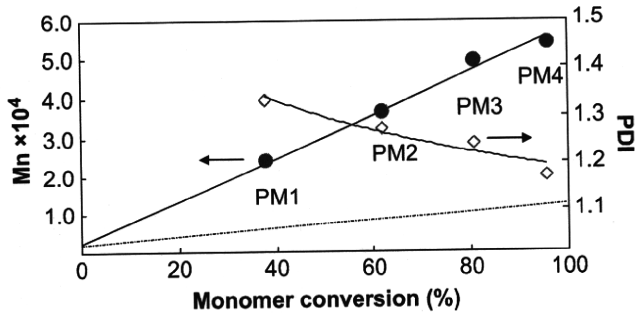

Fig. 2. Molecular weight and polydispersity plot against the monomer conversion. Synthesized block copolymer showed about five times higher molecular weight than the theoretical values, this was probably due to the end functionality of the PDMS macroinitiator. The dotted line represents Mn in the theoretical molecular weight.

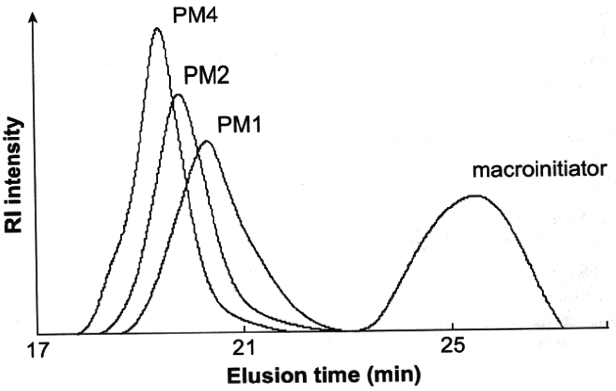

Fig. 3. SEC data of the PDMS/PMPC block copolymers.

Fig. 3 shows the SEC trace of the ATRP; it demonstrates that the overall block copolymer peaks remained monodal (Mw/Mn = 1.16) throughout the reaction, and the polymer peak continuously shifts to a higher molecular weight as monomer conversion increased. This indicates that all the radical species in the reacting mixtures are homogeneously participating in polymerization even two components shows large difference in solubility, thus block copolymers were successfully synthesized in well-controlled manner.

The overall information about the synthesized block copolymers is listed in Table 1.

3.2. Surface modification with block copolymers

3.2.1. Swelling–deswelling of PDMS substrates in mixed solvents

The surface modification of the PDMS substrate by using the swelling–deswelling method was carried out. Since all block copolymers are not dissolved in chloroform, a mixed solvent containing a good solvent for block copolymers should be used. Usually, the compositions of the mixed solvent play an important role in the swelling behavior of PDMS [29]. Thus we measured the swelling ratio of the PDMS substrate for various compositions of the mixed solvent, as shown in Fig. 4. As very well expected, the swelling ratio of the PDMS substrate decreased as the volume fraction of ethanol increased. Table 2 lists the solubility of the PDMS/PMPC block copolymers in various compositions of the mixed solvent. Based on this result, we selected a chloroform composition of 70 vol% for the

Table 1
Information about synthesized polymers

Polymer	MPC/PDMS repeating unit ratio[a]	Monomer conversion (%)	Reaction time (h)	Yield (%)	Mn × 10⁴		PDI
					SEC	NMR	
PM1	6.0	38	3	36	2.41	2.61	1.33
PM2	7.3	62	6	38.2	3.67	3.19	1.27
PM3	8.9	81	12	23.4	4.94	3.79	1.24
PM4	11.7	96	20	40.6	5.37	4.97	1.17
PMPC	–	100	24	51	5.24	–	1.33

[a] Repeating unit ratio was determined by NMR.

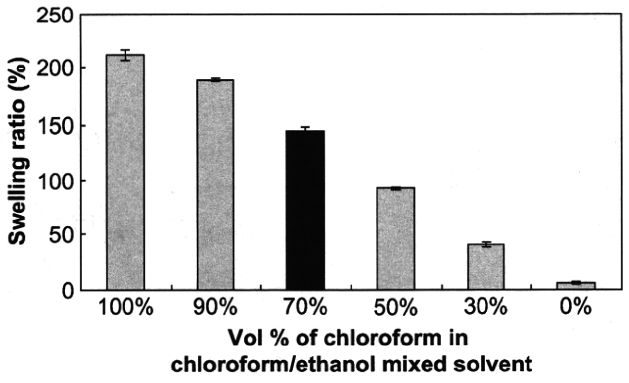

Fig. 4. Swelling ratio of PDMS substrate prepared in mixed solvent.

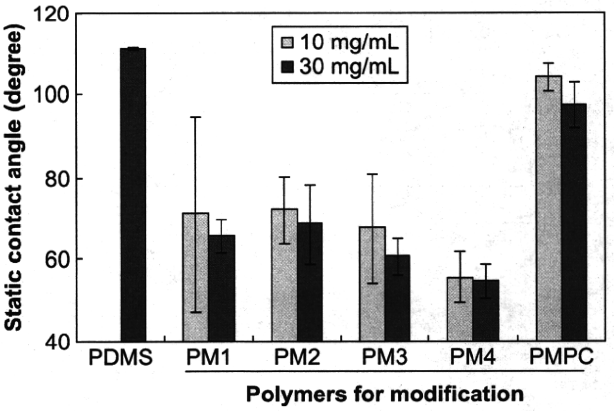

Fig. 5. Static contact angle of PDMS substrate treated and non-treated with the PDMS/PMPC block copolymer and PMPC.

mixed solvent in order to obtain both proper swelling ratio and good solubility for block copolymers.

3.2.2. Contact angle of modified PDMS substrates

The static contact angle measurement results are shown in Fig. 5. In all the samples, hydrophobic PDMS surfaces were converted to hydrophilic surfaces. However, we could not observe a significant concentration and molecular weight dependence of the PDMS/PMPC block copolymers on the contact angle. This is probably due to the limitation of the surface diffusibility of the PDMS substrate against the block copolymer; further researches are undergoing about this result. Even though, we could conclude that hydrophobic PDMS surfaces were successfully converted to hydrophilic surfaces by means of the simple swelling–deswelling method based on the fact that the overall values were half those of the non-treated PDMS substrate.

In order to confirm whether PDMS segments perform an active role in the hydrophilicity of PDMS in block copolymers or not, we synthesized PMPC that has almost the same molecular weight as the block copolymer with PM4. Fig. 5 also shows the contact angle comparison of the PDMS substrate treated with a block copolymer and PMPC. As shown in Fig. 5, there were almost no changes in the PDMS substrate treated with PMPC as compared to the non-treated one. This indicates that the PDMS segment in the block copolymer plays a dominant role in the surface modification of the PDMS substrate by the swelling–deswelling method. When PDMS substrate is swelled in proper solvent, large volume of inter space is generated by dimensional change. Thus the block copolymer segment positioned in or at the PDMS substrate (mainly PDMS segment) could be stably held by the shrinking force when the PDMS substrate is deswelled [20]. Hydrophobic interaction between PDMS segment and PDMS substrate make it more stable even that is in hydrophilic state such as biological environment. (About 80% of tethered segments were remained in water even after 2 months.) And this is thought as the reason why only PDMS containing block copolymers showed a tethering effect after aging in water. The overall mechanism is illustrated in Scheme 2. Due to the hydrophobic interaction, only the block copolymers could successfully tether the PMPC segment after penetrating into the substrate. (The fact that there was no physically adsorbed block copolymer was confirmed throughout the first contact angle measurement before aging in water, $110° \pm 2°$.)

Table 2
Solubility of synthesized block copolymers for various compositions of the mixed solvent

Polymer	Vol% of chloroform in chloroform/ethanol mixed solvent					
	100	90	70	50	30	0
PM4	−	−	+	+	+	+
PM3	−	−	+	+	+	+
PM2	−	−	+	+	+	+
PM1	−	+	+	+	+	+
PMPC	−	−	+	+	+	+

+: soluble; −: insoluble.

3.3. Surface characterization of modified PDMS

3.3.1. XPS characterization

The surfaces of the treated and non-treated PDMS substrates were analyzed using the atomic detection of C, O, N, and P by XPS. In all the cases of swelled–deswelled PDMS substrates with a block copolymer solution, the N and P components from the surface-tethered PMPC segments were detected at 402.5 eV and 134.0 eV, respectively (Fig. 6). On the other hand, no peak was detected in the non-treated PDMS substrate. This result indicates that the hydrophilicity of the swelled–deswelled PDMS substrate was due to the surface-tethered PMPC segments. The atomic percentage of P according to this result is shown in Fig. 7. This result clearly illustrates that the amount of P, which indicates the amount of PMPC segments on the surfaces, strongly depends on the concentration of the polymer solution rather than the molecular weight, i.e., a higher concentration leads to a larger number of phosphorylcholine groups on the PDMS surface. This result was expected because all the PDMS substrates showed almost the same swelling ratio regardless of the polymer concentration. This means that the possible amount of block copolymers passing into the swelled

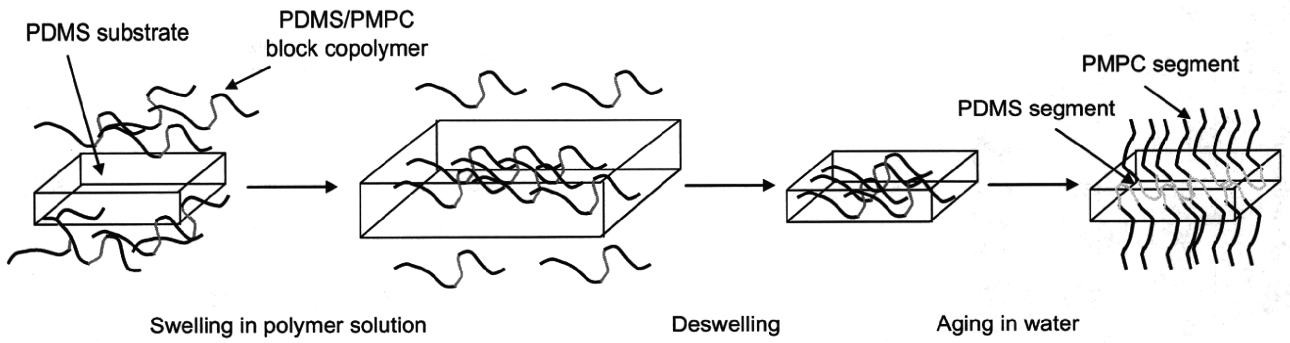

Scheme 2. Overall processing of surface tethering.

PDMS substrate was more in the 30 mg/mL polymer solution than that in the 10 mg/mL polymer solution; therefore, more PMPC segments are tethered onto the surfaces after aging in water.

3.3.2. AFM observation

The surface morphology of the modified PDMS substrate was observed under the wet condition by using AFM. Fig. 8 shows the topological images of the non-treated and representative-treated PDMS substrates. Different topological changes were clearly observed between the non-treated and treated PDMS substrates in 10 mg/mL and 30 mg/mL polymer solution. Based on the XPS analysis, it was thought that this difference was due to the surface-tethered PMPC segment. The difference in tethering density was also clearly observed by AFM (Fig. 8b, c). The root mean square roughness in 15 μm × 15 μm surface of a, b, and c was 1.3 nm, 4.0 nm, and 3.7 nm, respectively. This observed result is another evidence to make sure the polymer concentration is main variable in swelling–deswelling process. Generally, more densely tethered PMPC segments could more strongly prohibit protein adsorption, and this is considered to be reasonable based on the references because the larger amount of PMPC segments exhibits much thick hydrated layers around the phosphorylcholine groups [30,31]. This quantitative relationship between the amount of protein adsorption and the density of surface-tethered PMPC segments will be discussed below.

3.4. Biocompatibility evaluation

3.4.1. Protein adsorption test

The construction of a non-biofouling surface is the primary target to prepare biomaterials because most of the undesired bioreactions and bioresponses in artificial materials are promoted because of the adsorbed proteins [32,33]. Fig. 9 shows the result of the protein adsorption test calculated according to the micro-BCA experimental method. In most of the cases, the amount of adsorbed proteins decreased drastically as compared to that in the non-treated PDMS substrates. Note that the amount of adsorbed proteins on the PDMS substrate treated in the 10 mg/mL polymer solution was slightly greater than that treated in the 30 mg/mL polymer solution. This tendency is in

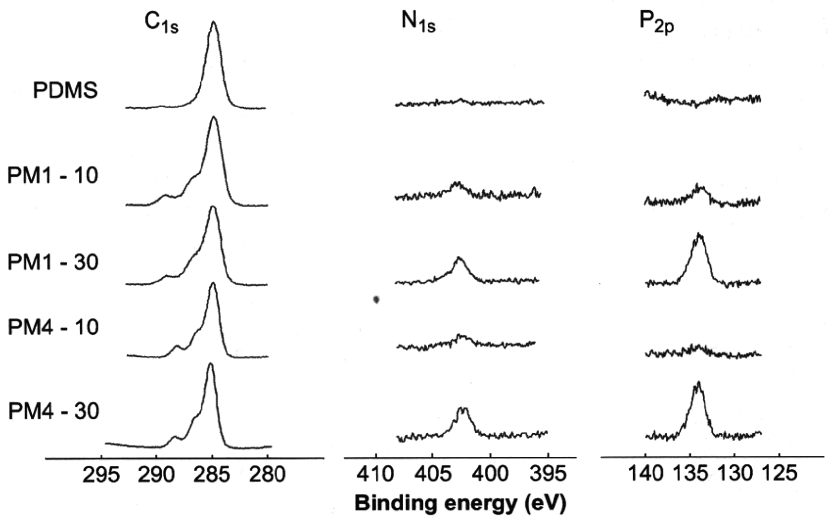

Fig. 6. XPS spectra of non-treated and treated PDMS substrates with PM1 and PM4. The marks of 10 and 30 indicate the concentration of the PDMS/PMPC block copolymer solution.

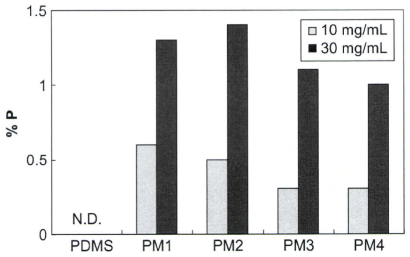

Fig. 7. Percentage of P on PDMS surfaces treated with PDMS/PMPC block copolymers with various concentrations. The percentage of P was calculated from the elements C, O, N, and P determined by the XPS measurement.

good agreement with the contact angle data, as shown in Fig. 5, and the results are discussed with the abovementioned XPS and AFM images. The fact that the phosphorylcholine groups in various materials preclude any protein adsorbing on the surface has been demonstrated by many researchers [34–36]. This phenomenon has been attributed to the large number of free water fractions around the phosphorylcholine groups. This makes the proteins contact with the material surface in a reverse manner without a significant conformational change [10]. Therefore, the more the phosphorylcholine groups on the PDMS substrate, the more the effect on the prevention of protein adsorption. In this research, we could confirm that the concentration control was efficient way to make more densely tethered surface, thus more anti-biofouling surface was formed.

3.4.2. L929 cell adhesion test

For most applications, biomaterials are generally in contact with the cells. Therefore, the interactions between the cells and biomaterials should be considered before they are used in various applications. Fig. 10 shows the optical microscope images of the PDMS substrates after performing the L929 cell adhesion test. Evidently, significant morphological differences were observed between the non-treated and treated PDMS substrate. A large number of cells were adhered to the non-treated substrate and most of these attached cells exhibited conformational changes, i.e., one of the states being attached, migrated, or grown. Contrary to this, the number of attached cells decreased significantly on the treated PDMS substrate. Moreover, the attached cells showed no conformational changes on both PDMS substrates modified in the 10 mg/mL and 30 mg/mL polymer solutions. This result indicated that the interactions between the cells and the PDMS substrate changed drastically, and it was thought to be caused by the surface-tethered PMPC segments. There are several

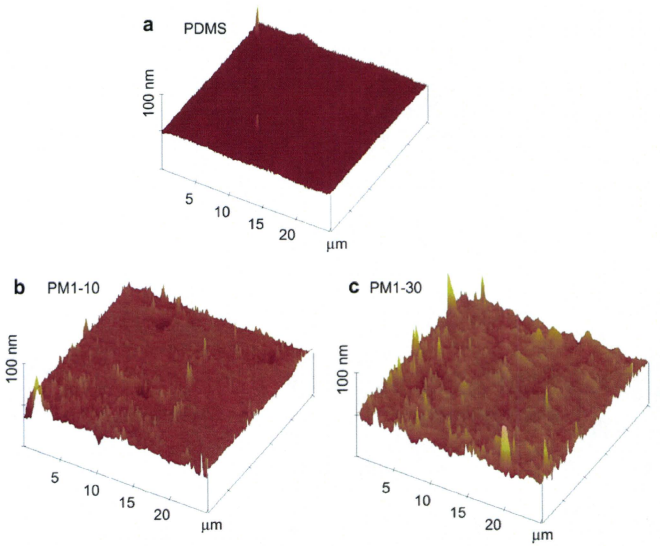

Fig. 8. AFM topological image of representative PDMS substrate treated with PM1 with various concentrations. The scan size is 25 μm × 25 μm and the height limitation is 100 nm.

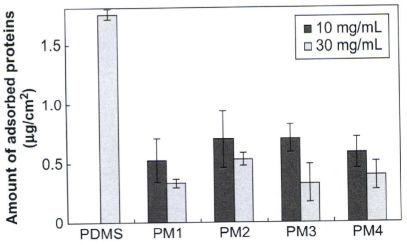

Fig. 9. Amount of protein adsorbed on the PDMS substrate treated with the PDMS/PMPC block copolymers with various concentrations.

factors to affect the cell adhesion behavior on the materials surface. Among these factors, mechanical property such as elastic modulus is recently reported important factor to directly affect the cell adhesion behavior. For example, Engler et al. [37] showed that the increased cell adhesion was related with the increased stiffness of substrate. Wong et al. [38] reviewed these relationships to suggest the necessity of the consideration of mechanical property of materials surface. Unfortunately, in this paper we could not discuss about the change in surface modulus caused by the PMPC tethering because that kind of research is now being carried out as other research field and not yet concluded. However, we speculated that the surface modification layer was very thin compared with the PDMS. That means the total mechanical properties of the modified PDMS did not change dramatically. Thus in this paper, we discuss the cause of decrease in cell adhesion in the point of cell–protein interaction. Cell interactions under external conditions are mediated by receptors in the cell membrane, which interact with the proteins and other ligands that adsorb onto the material surface from the surrounding plasma and other fluids. When the materials are surrounded by body fluids, the surface is rapidly covered with proteins. The nature of these adsorbed proteins is controlled by the characteristics of the material surface and these controlled proteins markedly enhance cell attachment, migration, and growth [5]. Since the large amount of free water around the PMPC segment precludes the adsorption and conformational changes in proteins at the material surface as discussed above, no significant interactions between the receptors in the cell membrane and adsorbed proteins were expected. Further, this is considered to be the reason why significant morphological changes were observed between the cells on treated and non-treated PDMS substrates.

4. Conclusions

Hydrophobic and biofouling PDMS surfaces were successfully modified by using block copolymers comprising PMPC and PDMS. PDMS blocks play a dominant role in surface

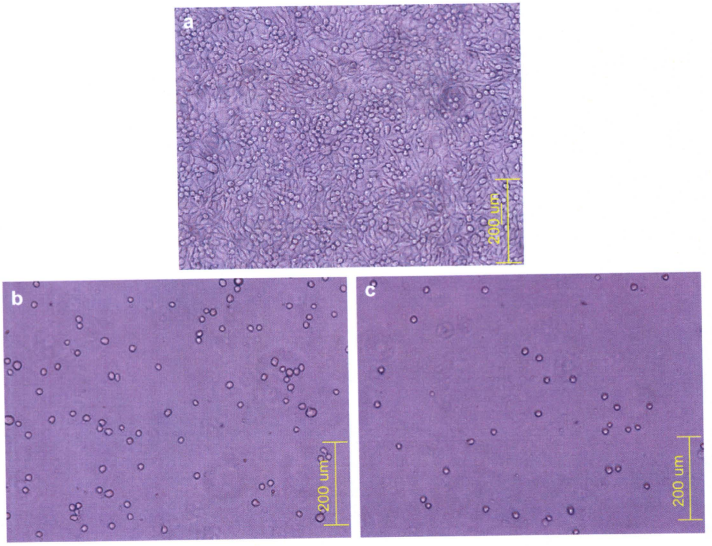

Fig. 10. Optical microscope images of PDMS substrate treated with the PDMS/PMPC block copolymer after 1-day adhesion test with L929 cells. Images of the unmodified PDMS substrate (a), PDMS substrate modified in 10 mg/mL (b) and 30 mg/mL (c) PM1 polymer solutions, respectively.